J|A|C|S COMMUNICATIONS

Published on Web 12/04/2009

# Analysis of an Anomalous Mutant of MutM DNA Glycosylase Leads to New Insights into the Catalytic Mechanism

Kwangho Nam,[†] Gregory L. Verdine,*[,†,‡,§,||] and Martin Karplus*[,†,⊥]

*Departments of Chemistry and Chemical Biology, Molecular and Cellular Biology, and Stem Cell and Regenerative Biology, Harvard University, Cambridge, Massachusetts 02138, Chemical Biology Initiative and Program in Cancer Chemical Biology, Dana-Farber Cancer Institute, Boston, Massachusetts 02115, and L'Institut de Science et d'Ingénierie Supramoléculaires (ISIS), Université Louis Pasteur, 8 allée Gaspard Monge, 67000 Strasbourg, France*

Received September 6, 2009; E-mail: verdine@chemistry.harvard.edu; marci@tammy.harvard.edu

Lesion-specific DNA glycosylases play the key role in base-excision DNA repair of finding the damaged base and catalyzing its removal.[1−3] Structural,[4−6] computational,[6,7] and experimental studies[8,9] have shown that when MutM, a bacterial DNA glycosylase specific for 8-oxoguanine (oxoG), encounters an oxoG lesion, the damaged nucleobase is extruded from the DNA and inserted into the enzyme active site, whereupon catalysis of glycosidic bond cleavage ensues. Potential of mean force (pmf) calculations[6] making use of X-ray crystal structures of MutM bound to DNA containing either an extrahelical oxoG bound in the enzyme active site[4,5] or an intrahelical oxoG[6] or G[4] have shown that the free-energy barrier for extrusion of oxoG is 7 kcal/mol lower than that for G. To obtain a crystal of a "lesion-recognition" complex (LRC) with oxoG in the active site of MutM bound to DNA,[5] the catalytically essential Glu3 (E3) residue was mutated to Gln (Q) ($MutM^{E3Q}$)[10] (Figure 1). In the pmf simulations, the Q3 residue was restored computationally to E3 to obtain the wild-type enzyme ($MutM^{WT}$). The simulations indicated that extrusion of the oxoG into the active site was disfavored by ∼5 kcal/mol relative to the intrahelical state. Why then had it been possible to crystallize such an apparently disfavored LRC? Here we show that the E3Q mutation provides substantial stabilization of oxoG in the active site of MutM. The simulations further show that oxoG is stabilized in the active site by protonation of the E3 carboxyl group during the insertion process. It is also pointed out that the protonation could be significant for base-excision catalysis. The results highlight the importance of accounting for the potential energetic and structural effects of mutations frequently introduced into enzymes to capture otherwise fleeting intermediates.[11,12]

Pmf simulations[13] of the extrusion of oxoG by $MutM^{E3Q}$ were performed using the method described previously[6] for $MutM^{WT}$ [see the Supporting Information (SI)]. Figure 2 and Figure S1 in the SI compare pmf profile for $MutM^{E3Q}$ with that for $MutM^{WT}$ having E3 deprotonated (denoted as E3-$COO^-$). The free energy for oxoG extrusion into the active site of $MutM^{E3Q}$ is reduced by a significant amount (−14.7 kcal/mol) relative to that for $MutM^{WT}$, so oxoG is more stable in the active site of the E3Q mutant than in the intrahelical configuration, in agreement with experiment. The shapes of the two-dimensional pmf's for the WT and the E3Q mutant are also different (Figure 2). For $MutM^{WT}$, the rate-limiting barrier (11 kcal/mol at $TS_2$) is for the anti to syn rotation of the glycosidic bond, while for $MutM^{E3Q}$, the rotation after extrusion occurs without a barrier, and the free energy decreases continuously until oxoG is in the enzyme active site. The barrier for the first step ($TS_1$), corresponding to extrusion of the base through the minor groove, is 4.2 kcal/mol for $MutM^{WT}$ and 8.7 kcal/mol for $MutM^{E3Q}$. Pmf simulations for G extrusion show that the E3Q mutation also reduces the free energy for binding of G to the active site to −12.1 kcal/mol relative to that of the intrahelical conformation.

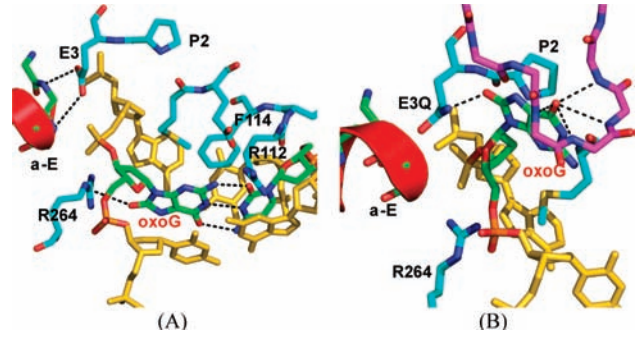


***Figure 1.*** Comparison of the MutM structures of (A) the encounter complex (EC) and (B) the lesion recognition complex (LRC). The oxoG-capping loop in the LRC is shown with purple sticks and the α-E helix as a red cartoon. In the base-extrusion process, oxoG is rotated along its glycosidic bond to the syn conformation.

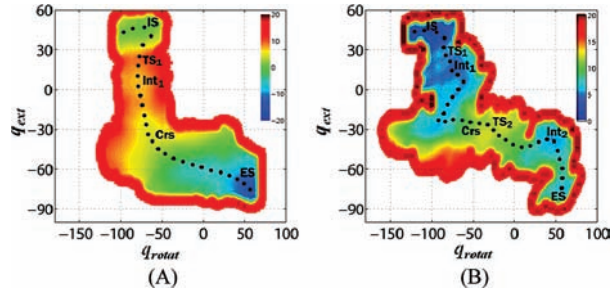


***Figure 2.*** Computed potentials of mean force for oxoG extrusion, rotation, and entrance into the active site of (A) $MutM^{E3Q}$ and (B) E3-$COO^-$ $MutM^{WT}$. The pseudodihedral angles for the base extrusion and rotation are $q_{ext}$ and $q_{rotat}$, respectively, which represent the extrusion of oxoG into the active site from the intrahelical state (IS) to the active-site bound state (ES); for the definitions of the pseudodihedral angles, see Figure S2. Along the minimum free-energy paths (shown by black dots), several key points are indicated: transition states ($TS_1$ for base extrusion from the DNA helix and $TS_2$ for base rotation), intermediate states ($Int_1$ for the extrahelical base and $Int_2$ for the state where oxoG forms a hydrogen bond with P2),[6] and the crossover point (Crs) (see Figure 3). The units of the dihedral angles and the free energy are degrees and kcal/mol, respectively.

Alchemical free-energy simulations using $\lambda$-dynamics-based thermodynamic integration (TI)[6,14,15] were carried out to check the pmf results. The TI values confirmed that the E3Q mutation significantly lowers the free energies for both oxoG and G binding in the enzyme active site (see Table S1). Free-energy component

[†] Department of Chemistry and Chemical Biology, Harvard University.
[‡] Department of Molecular and Cellular Biology, Harvard University.
[§] Department of Stem Cell and Regenerative Biology, Harvard University.
[||] Dana-Farber Cancer Institute.
[⊥] Université Louis Pasteur.



10.1021/ja907544b 

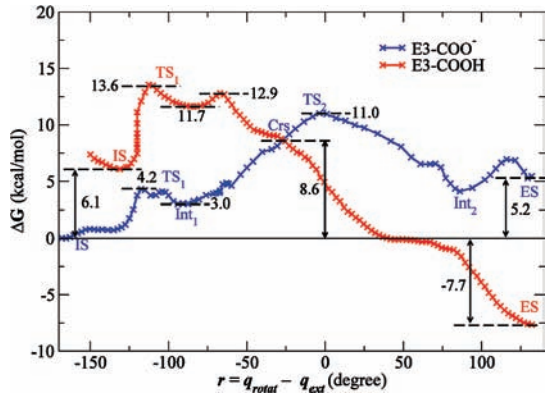


***Figure 3.*** Potentials of mean force along a progress variable ($r$) equal to the difference of $q_{rotat}$ and $q_{ext}$ for oxoG extrusion by MutM$^{WT}$ with a protonated (red) or deprotonated (blue) E3 residue. The profiles for E3-COOH are shifted upward by 6.1 kcal/mol, the free energy required to protonate the E3 residue at pH 7 (see the SI). Indicated points correspond to points labeled in Figure 2 and Figure S5. The zero of free energy is that of the intrahelical state (IS).

analysis[16] (Figure S3) further showed that the dominant destabilization arises from deprotonated E3 in the active site, which interacts repulsively with the extruded oxoG and neighboring phosphate groups. These interactions are less repulsive for Q3, as expected.

The above results raise the question of why oxoG is favored in the active site of the WT enzyme. One possibility is that E3 becomes protonated when oxoG enters the active site, although it has been assumed that this residue is deprotonated at pH 7. The crystal structure suggests that the repulsive interactions between E3-COO$^-$ and phosphate groups of DNA[5] could be diminished by neutralization of the negative charge on E3. Furthermore, a hydrogen bond between protonated E3 (denoted as E3-COOH) and the 8-oxocarbonyl of the extrahelical oxoG can be formed in the active site; this is analogous to the hydrogen bond formed between 8C═O and the side-chain $NH_2$ group of Q3. The free-energy profiles for extrusion of oxoG by E3-COO$^-$ and E3-COOH are shown in Figure 3 (the corresponding results for G are shown in Figure S4). The two pmf profiles cross at an early stage of the base rotation; the progress variable $r$ defined in the figure is equal to $-26°$ for oxoG and $-24°$ for G at the crossover point (denoted as Crs in Figure 3 and Figure S4). Since the system can cross from one free-energy surface to the other by proton transfer, the free energy for oxoG extrusion into the active site is $-7.7$ kcal/mol (with E3-COOH), and the rate-limiting barrier is at Crs (8.6 kcal/mol). Protonation of the E3 residue also stabilizes G in the active site, but G is still more stable in the intrahelical state (0.6 kcal/mol), and the free-energy barrier for its extrusion is 11.0 kcal/mol at the Crs. TI simulations for the protonation of E3 were consistent with the results from pmf simulations (Table S2).

In the search of the DNA for the damaged base by MutM, a fast oxoG recognition mechanism is required because of the high speed at which MutM slides along DNA.[9] Previous results[6] have shown that the initial extrusion of the base through the minor groove of the DNA helix is indeed fast and kinetically discriminates oxoG from G. The present results suggest that there also could be a thermodynamic discrimination step in the active site. If E3 becomes protonated, the free energy for binding of the extruded oxoG in the active site is favorable ($-7.7$ kcal/mol; Figure 3), while it remains unfavorable for G (0.6 kcal/mol; Figure S4). The calculated effects correspond to a difference by a factor of $10^8$ in the equilibrium constants for oxoG and G in the active site. The results suggest the following sequence of events for extrusion of oxoG into the active site: (1) E3 is initially deprotonated when oxoG is extruded from the DNA ($TS_1$ barrier of 4.2 kcal/mol); (2) once the system reaches an intermediate extrahelical state ($Int_1$, 3.0 kcal/mol), oxoG begins rotating around its glycosidic bond, and E3 becomes protonated (Crs, at the crossover point of 8.6 kcal/mol); and (3) oxoG enters the active site without any additional barriers. There are a number of waters in the protein−DNA interface[4,6] that could serve as the source of the proton; also, Pro2, which has to be deprotonated to be a nucleophile, could provide the proton through a water chain near the interface.[17]

In the present study, we have investigated the effect of the alterations of the key residue E3 in MutM on the free energy along the nucleobase extrusion pathway. We conclude that the E3Q mutation favors oxoG binding in the enzyme active site over binding of the WT enzyme. Analyses of the computed free energies for MutM$^{WT}$ have provided new insights into the role of the E3 residue in base extrusion and recognition of a damaged nucleobase. The similarity between the side chains of Q and protonated E and the pmf simulations suggest that MutM exploits a two-step discrimination mechanism: fast kinetic discrimination at the early stage of damaged-base recognition and thermodynamic discrimination via protonation of the E3 residue, which favors binding of oxoG in the active site. The glycosyl transfer reaction has been suggested to occur via an $S_N1$-like displacement of oxoG by the nucleophile Pro2;[5] if protonated, E3 would facilitate the reaction by activating the oxoG leaving group, for example, through the protonation at O8, and subsequently by stabilization of the oxocarbenium ion. Further experimental and computational studies are required in order to confirm the present results concerning lesion recognition and catalysis by this important enzyme.

**Acknowledgment.** This work was supported by grants from NIH to G.L.V. (CA100742) and M.K. (GM030804) and by a postdoctoral fellowship from National Cancer Center to K.N. NERSC and FAS at Harvard University provided computing resources. K.N. acknowledges Drs. J. Pu, V. Ovchinnikov, G. Zheng, and M. Spong and Ms. Y. Qi for helpful discussion.

**Supporting Information Available:** Computational details and supporting tables and figures. This material is available free of charge via the Internet at http://pubs.acs.org.

## References

(1) Lindahl, T.; Wood, R. D. *Science* **1999**, *286*, 1897.
(2) Krokan, H. E.; Nilsen, H.; Skorpen, F.; Otterlei, M.; Slupphaug, G. *FEBS Lett.* **2000**, *476*, 73.
(3) Fromme, J. C.; Banerjee, A.; Verdine, G. L. *Curr. Opin. Struct. Biol.* **2004**, *14*, 43.
(4) Banerjee, A.; Santos, W. L.; Verdine, G. L. *Science* **2006**, *311*, 1153.
(5) Fromme, J. C.; Verdine, G. L. *J. Biol. Chem.* **2003**, *278*, 51543.
(6) Qi, Y.; Spong, M.; Nam, K.; Banerjee, A.; Jiralerspong, S.; Karplus, M.; Verdine, G. L. *Nature* **2009**, in press (Dec 10).
(7) Song, K.; Kelso, C.; de los Santos, C.; Grollman, A. P.; Simmerling, C. *J. Am. Chem. Soc.* **2007**, *129*, 14536.
(8) Minetti, C. A. S. A.; Remeta, D. P.; Breslauer, K. J. *Proc. Natl. Acad. Sci. U.S.A.* **2008**, *105*, 70.
(9) Blainey, P. C.; van Oijen, A. M.; Banerjee, A.; Verdine, G. L.; Xie, X. S. *Proc. Natl. Acad. Sci. U.S.A.* **2006**, *103*, 5752.
(10) Lavrukhin, O. V.; Lloyd, R. S. *Biochemistry* **2000**, *39*, 15266.
(11) Fersht, A. R.; Winter, G. *Ciba. Found. Symp.* **1985**, *111*, 204.
(12) Fersht, A. R. *Structure and Mechanism in Protein Science: A Guide to Enzyme Catalysis and Protein Folding*; W. H. Freeman: New York, 1999.
(13) Torrie, G. M.; Valleau, J. P. *J. Comput. Phys.* **1977**, *23*, 187.
(14) Kong, X.; Brooks, C. L., III. *J. Chem. Phys.* **1996**, *105*, 2414.
(15) Kollman, P. A. *Chem. Rev.* **1993**, *93*, 2395.
(16) Boresch, S.; Karplus, M. *J. Mol. Biol.* **1995**, *254*, 801.
(17) Cui, Q.; Karplus, M. *J. Phys. Chem. B* **2003**, *107*, 1071.

JA907544B